Unsteady Turbulent Boundary Layers in Two-Dimensional, Incompressible Flow

JOHN F. NASH*
Sybucon Inc., Atlanta, Ga.
LAWRENCE W. CARR†
U.S. Army Air Mobility Research and Development Laboratory, Ames Directorate, Moffett Field, Calif.
AND
ROBERT E. SINGLETON‡
Lockheed-Georgia Company, Marietta, Ga.

This paper presents the results of some calculations aimed at studying the characteristics of turbulent boundary layers in unsteady flow. The calculations were performed using the method of Singleton and Nash, which is based on the turbulent kinetic energy equation. Emphasis is placed on the approach to zero wall stress, and the results show the extent to which onset of this condition can be delayed by the effects of time dependence. The delay is not associated merely with alleviation of the pressure gradients, and quasi-steady methods cannot readily be used to calculate this type of flow.

Nomenclature

A, A_o, A_1 = constants in external velocity definitions
a_1, a_2 = constants in turbulence energy equation
c = chord length of the plate, assumed to be unity
L = dissipation length
P = period of the motion
p = static pressure
R = ratio of local acceleration to substantial acceleration
t = time
U = chordwise ensemble average velocity
u = chordwise random fluctuation about U
V = normal ensemble average velocity
v = normal random fluctuation about V
W = lateral ensemble average velocity
w = lateral random fluctuation about W
uv = ensemble average of the product uv
x = distance measured in chordwise direction
y = distance measured normal to wall
z = distance measured laterally
δ = boundary-layer thickness
δ^* = boundary-layer displacement thickness
ρ = density
τ = shear stress
ω = frequency parameter

Subscripts

e = value at the outer edge of boundary layer
w = value at wall
o = reference value

Presented as Paper 73-650 at the AIAA 6th Fluid and Plasma Dynamics Conference, Palm Springs, Calif., July 16–18, 1973; submitted August 2, 1973; revision received August 2, 1974. This research was supported by the U.S. Army Air Mobility Research and Development Laboratory, Moffett Field, Calif., under Contract NAS2-6466. The authors are indebted to V. C. Patel of the University of Iowa, who served as a consultant on the program, for many helpful discussions during the course of the work.

Index categories: Boundary Layers and Convective Heat Transfer—Turbulent; Nonsteady Aerodynamics.

* Consultant to the Lockheed-Georgia Company.
† Research Scientist. Member AIAA.
‡ Presently Chief, Fluid Mechanics Branch, Army Research Office, Durham, N.C.

Introduction

THE subject of unsteady turbulent boundary layers is of substantial interest from both the fundamental and the practical standpoints. On the one hand, study of this subject adds an important new dimension to the already large and complex area of research on general turbulent flows. On the other, work on the effects of time dependence on turbulent boundary-layer development has been found to be crucial to the solution of a number of pressing engineering problems.

Among current problems of this type are the flows over the blades in compressors and turbines and over the aerodynamic surfaces of vehicles in maneuvering flight, particularly remotely piloted vehicles that are often subject to larger rates of acceleration than manned aircraft. Another especially conspicuous problem at this time is the flow over a helicopter rotor in translating motion. It has long been suspected that the effects of time dependence in the boundary layer have an important influence on rotor performance, and the pessimistic results of quasi-steady calculations for a typical rotor[1] added considerable weight to these suspicions.

The subject of unsteady boundary layers is in its infancy, and the subject of unsteady *turbulent* boundary layers was virtually untouched until the last 3 to 4 years. Since then, the differential method of Patel and Nash[2] and the integral method of McDonald and Shamroth,[3] for calculating two-dimensional flows with both spatial and temporal variations, have been published. A few other methods have also appeared which treat only temporally varying flows. Recently, the method of Patel and Nash has been refined by the inclusion of a more accurate numerical scheme and extended to cover infinite-yawed-cylinder flows. The new method[4,5] is used as the basis for the present calculations, although only two-dimensional flows are considered here.

The objective of the present work was to perform numerical experiments to explore some of the properties of time-dependent turbulent boundary layers. The flows considered are idealized, but their broad character and the time rates of change assumed are relevant to a number of engineering problems, including the helicopter rotor problem.

Specifically, this study concentrated on the effects of time dependence on the onset of flow reversal at the wall: the condition where the wall shear stress just reaches zero. It should be emphasized that, in unsteady flows, this condition does not

imply separation in the sense of detachment of the outer potential flow from the body; these are distinct phenomena. In the types of unsteady flow considered, separation *per se* was not observed; it would have been expected to occur later than reversal, but the calculations did not extend beyond the onset of flow reversal. Further studies are in progress to explore the characteristics of the flow between reversal and separation. The usual assumption was made that the boundary layer can be uncoupled from the external flow. This assumption can be questioned near a separation point; however, as noted, separation did not occur in the flows considered. Near a point of flow reversal, the assumption is evidently more secure in these unsteady flows than it would be in comparable steady flows.

It was also considered important to try to determine the range of validity of quasi-steady methods. Time-dependent calculations are more difficult to perform and are more expensive to perform than steady ones, and it is useful to know the point, in terms of increasing unsteadiness of the flow, beyond which the added complexity and expense have to be incurred to obtain valid results.

Governing Equations of the Method

This paper is concerned with the turbulent boundary layer in incompressible, time-dependent flow. Only two-dimensional flows are considered here although, as remarked earlier, the calculation method used[5] extends to infinite-yawed-cylinder flows also. The equations are formulated in terms of a rectangular coordinate system with x measured in the stream direction, y measured normal to the surface, and z measured laterally.

The velocities in the x, y, and z directions are expressed in the form $U+u$, $V+v$, $W+w$, respectively, where U, V, u, v, and w are all functions of x, y, and t. The term W is identically zero by virtue of the assumption of two-dimensionality, and all derivatives with respect to z are also zero. The components of velocity U, V, and W are defined as ensemble averages taken over a large number of realizations of the same basic flow, or successive flows with the same time history and the same boundary conditions, e.g., successive cycles of a stable oscillatory flow. The components u, v, and w represent the random fluctuations about U, V, and W, and by implication the ensemble averages of u, v, and w are identically zero.

The equations of motion for a flow of the type described above can be derived from the time-dependent, Navier-Stokes equations by replacing the three velocity components by $U+u$, $V+v$, and $W+w$ (as defined above) and forming the ensemble average. Introduction of the boundary-layer approximation and restriction to flows with $W=0$ and zero z derivatives then yields the momentum equation for U:

$$\frac{\partial U}{\partial t}+U\frac{\partial U}{\partial x}+V\frac{\partial U}{\partial y}+\frac{1}{\rho}\frac{\partial p}{\partial x}+\frac{\partial}{\partial y}(\overline{uv})=0 \qquad (1)$$

together with the statement that the pressure is constant through the boundary layer. In the momentum equation, $\overline{uv}$ is the ensemble average of the product uv, and has essentially the same meaning as the Reynolds stress appearing in the steady turbulent boundary-layer equation. Thus, the shear stress $\tau=-\rho\overline{uv}$. The continuity equation retains its usual form:

$$\partial U/\partial x+\partial V/\partial y=0 \qquad (2)$$

The above equations are identical in form to the ones that would have been derived if U, V, and W had been specified as time averages. They are identical in substance, too, if the assumption of ergodicity holds, which requires that the time scale of the turbulent motion be short compared with the time scale of the motion as a whole. A number of flows of practical interest involve unsteadiness of the boundary conditions which is too rapid for an adequate distinction to be made, particularly when due attention is paid to the importance of the large-eddy motions in the boundary layer. These motions can have a time scale comparable to the time taken for a particle to be convected a distance many times the boundary-layer thickness. To state that the equations involve ensemble-average, rather than time-average quantities, does not mean that ensemble averages cannot be *approximated* by time averages. The important point to be made, at this stage, is that the equations are most secure when viewed as ensemble-average equations.

The turbulent shear stress is assumed to behave according to the rate equation used in the method for steady flows,[6,7] but with the convective derivative extended to include the time derivative:

$$\frac{\partial}{\partial t}(\overline{uv})+U\frac{\partial}{\partial x}(\overline{uv})+V\frac{\partial}{\partial y}(\overline{uv})-2a_1\left[\overline{uv}\frac{\partial U}{\partial y}-\frac{\partial}{\partial y}(a_2\overline{uv})+\frac{(-\overline{uv})^{3/2}}{L}\right]=0 \qquad (3)$$

This equation, first proposed by Bradshaw et al.,[8,9] is derived from the turbulent kinetic-energy equation by postulating proportionality between shear stress and turbulent intensity, and by appropriate modeling of the diffusion and dissipation terms. Extensive comparisons with experiment for both two- and three-dimensional flows have been made for the steady case and have confirmed the basic adequacy of the model. There is, as yet, no direct evidence of its adequacy for the unsteady case. The functions a_1, a_2, and L are assumed to be the same functions as appear in the steady-flow method[6,7]: a_2 and L are shown in Fig. 1, and $a_1=0.15$. This assumption implies that a) the ensemble-average quantity $\overline{uv}$ behaves in the same way as the time-average Reynolds stress in steady flow, and b) that time dependence in the mean flow has a negligible effect on the structure of the turbulence. Neither hypothesis has been verified experimentally and, clearly, there is an urgent need to do so. For the present, these hypotheses are necessary to proceed at all, but it must be stressed that some of the conclusions from this study may need revision if later experimental work shows that certain underlying assumptions in the method are seriously in error.

The governing equations, consisting of the momentum, continuity, and shear stress-equations given above, are integrated in a three-dimensional domain (two space dimensions and time) by an explicit finite-difference method. As in the method of Ref. 2, integration proceeds in the time direction. At each time level, the calculation yields profiles of ensemble-average velocity, U, and shear stress, $\overline{uv}$, vs y, at prescribed x stations. Details of the calculation method are given in Refs. 4, 5.

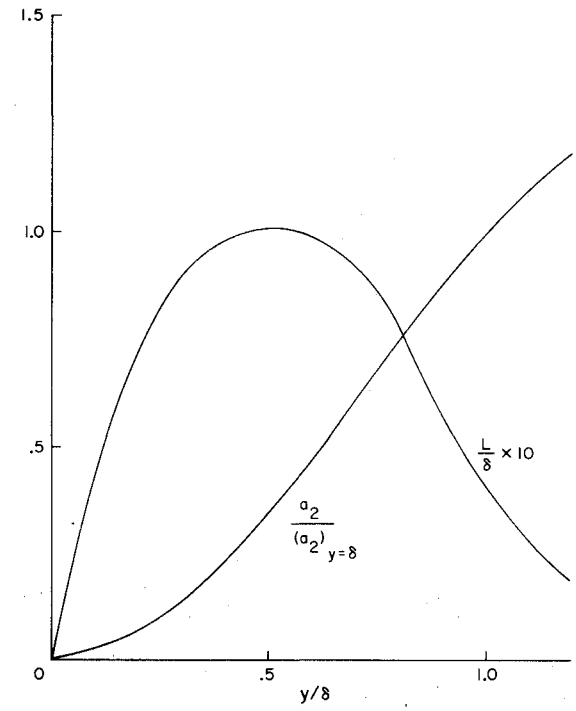

Fig. 1 Empirical functions.

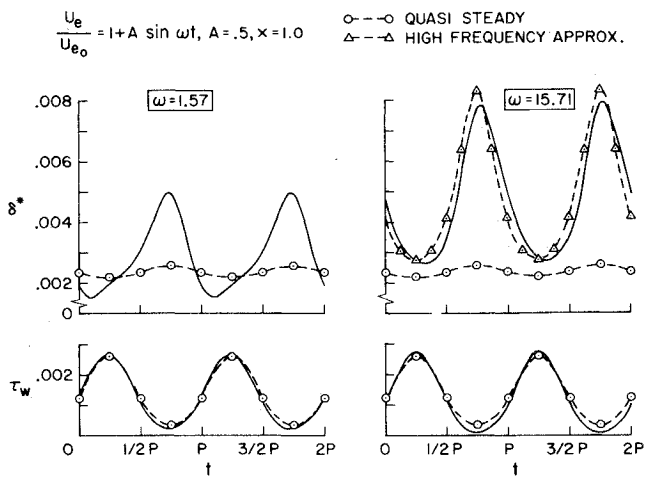

Fig. 2 Oscillatory flow over a flat plate, Flow A.

Computational Experiments

The properties of time-dependent, turbulent boundary layers were studied by conducting computational experiments in which the boundary-layer development was calculated for a range of external velocity distributions. Five flow situations were selected, designated flows A through E, and calculations were done for each flow for a range of the relevant parameters.

Flows A and B were oscillatory flows, on a flat plate and with a mean retardation, respectively:

$$\text{Flow A:} \qquad U_e = U_{e_0}(1 + A\sin\omega t) \tag{4}$$

$$\text{Flow B:} \qquad U_e = U_{e_0}[1 + (A_0 + A_1\sin\omega t)x] \tag{5}$$

Flows C and D were monotonically time varying, with external velocity distributions defined as:

$$\text{Flow C:} \qquad U_e = U_{e_0}(1 - \omega t x) \tag{6}$$

$$\text{Flow D:} \qquad U_e = U_{e_0}[1 + \omega t(1 - x)] \tag{7}$$

Flow E was the same as Flow D up to some time t_f, but for $t > t_f$, the external velocity distribution was frozen, allowing a relaxation of the boundary layer toward retarded steady-state conditions.

In all the calculations, the Reynolds number, based on U_{e_0} and the chord of the plate, over which the flow was developing, was taken to be 10^7. The boundary condition at $x = 0$ was set by taking

$$\delta_0(t) = 0.00444(U_e/U_{e_0})^{-0.2} \tag{8}$$

and appropriately scaling flat-plate velocity and shear-stress profiles on that thickness (δ_0 is normalized by the length of the plate). The above condition corresponds to the assumption that a steady flat-plate boundary layer had developed over a constant length, upstream of $x = 0$, at the instantaneous velocity U_e.

For the following results, lengths are made dimensionless by dividing by the length of the plate, velocities by dividing by U_{e_0}, and shear stresses by dividing by $\rho U_{e_0}^2$. Time is made dimensionless by multiplying by U_{e_0} and dividing by the length of the plate. For the oscillatory flows, a reduced frequency, ω, is defined as

$$\omega = 2\pi/P \tag{9}$$

where P is the period of the motion in time units. If $\omega = 2\pi$, a complete cycle occurs in the time taken for a fluid particle, moving with velocity U_{e_0}, to be convected the length of the plate. In the monotonically time-varying flows, ω is retained as a measure of the rate distortion of the flow, i.e., $1/\omega$ is a characteristic time of the motion.

For comparison with the fully time-dependent calculations, quasi-steady calculations were also performed. In the latter, the time scale of the motion was allowed to tend to infinity, corresponding to the limit $\omega \to 0$. In a few cases, the calculations were performed using the unsteady method and relaxing toward the quasi-steady solution in the limit $t \to \infty$. This procedure was expensive in terms of machine time, and most of the calculations were done by integrating the governing equations, with the t derivatives omitted, by a conventional forward-marching procedure advancing in the x direction. The results of the more economical scheme were virtually identical to those obtained by the full time relaxation.

In the quasi-steady calculations, the external velocity distribution was taken to be the same as that which would have occurred if the unsteady flow had been frozen at that particularly instant of time. For comparison with a given time-dependent flow, several quasi-steady calculations needed to be performed, each corresponding to a different point in time. In all cases, the quasi-steady calculations excluded unsteadiness completely; the use of an "effective" pressure gradient, which includes the term $\partial U_e/\partial t$ in the momentum equation, was not attempted. Such an approach leads to a significant inconsistency between the apparent pressure distribution and the actual velocity distribution: they no longer mutually satisfy Bernoulli's equation. In any case, as will be shown later, it can also lead to results that contradict those obtained by solving the full unsteady boundary-layer equations.

Oscillatory Flows

The results for Flow A, the oscillatory flow over a flat plate, are presented more fully in Ref. 5, and the reader will find additional details there. It was observed that the wall shear stress was represented well by quasi-steady calculations, except when τ_w became small. Even then, the quasi-steady predictions were surprisingly good over much of the cycle; however, the minimum values of τ_w predicted by the quasi-steady model were too high. This latter situation was to be expected because incipient flow reversal ($\tau_w = 0$) can occur in the unsteady flow if A or ω are large enough, but it could never be predicted by the quasi-steady model unless A were so large as to stagnate the external flow.

The displacement thickness was not approximated adequately by quasi-steady calculations even at relatively low frequencies ($\omega = 1.57$). On the other hand, a "high-frequency approximation," in which it was assumed that $U_e - U$ would be constant across the boundary layer, yielding $U_e\delta^* = $ constant, was found to give reasonable results (Fig. 2). Some data on the phase angles between τ_w, δ^*, and U_e are presented in Ref. 5.

The retarded oscillatory flow. Flow B, exhibits some important contrasts with Flow A. With $A_0 = 0.2$ and $A_1 = 0.4$, the unsteady flow comes close to incipient reversal ($\tau_w = 0$) near the "bottom" of the cycle (Fig. 3). However, the equivalent quasi-steady flow actually separates during that part of the cycle. Thus the unsteady boundary layer manages to avoid flow reversal

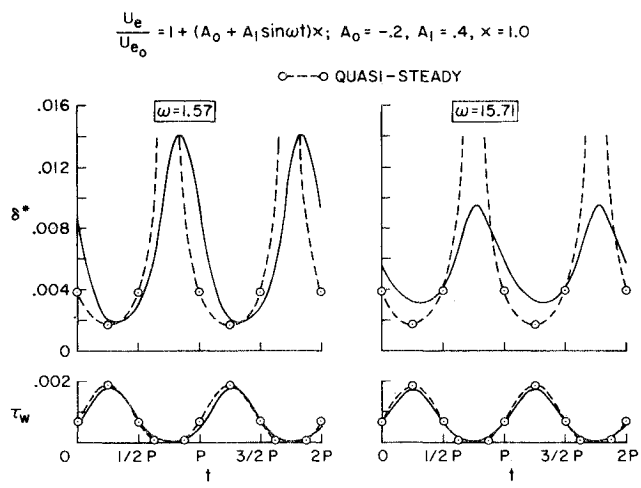

Fig. 3 Oscillatory retarded flow, Flow B.

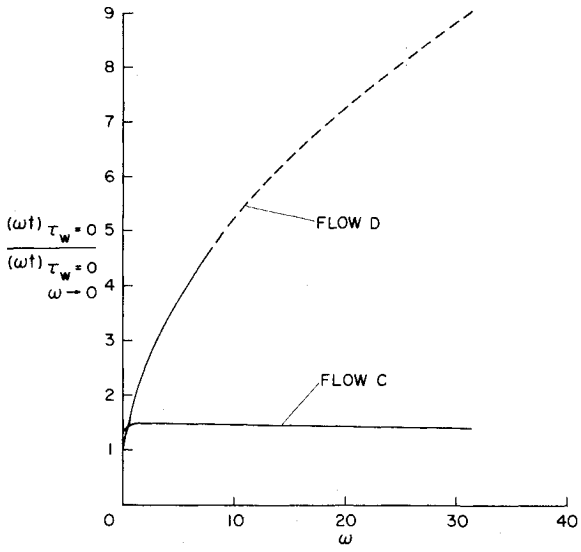

Fig. 4 Variation of velocity gradient magnitude for incipient reversal at $x = 1$ vs frequency.

throughout the cycle, even though the maximum instantaneous retardation would be enough to cause separation if it were maintained for a long time. It is significant that, in the present case, the effect of time dependence is to delay the onset of flow reversal, whereas for the oscillating plate (Flow A), time-dependent effects cause the separation to occur.

In Fig. 3, over the part of the cycle where the quasi-steady calculation indicates separation, the quasi-steady values of δ^* are large or infinite. The unsteady values, in contrast, are well behaved throughout the cycle. Again, if points close to zero wall shear stress are excluded, it is remarkable how good an approximation the quasi-steady wall shear stress values are to the unsteady values for a wide range of both frequency and amplitude.

Monotonically Time-Varying Flows

In the three monotonically time-varying flows (Flows C, D, and E), only positive values of ω and t were considered, and so all three flows involved decelerating external flows. In Flow C, the external velocity distribution pivoted about the leading edge of the plate ($x = 0$), and this flow might be regarded as an idealized model of the flow in a channel with one wall flexing and rotating outward. In Flows D and E, the external velocity distribution pivoted about the trailing edge of the plate ($x = 1$), and these flows might be regarded as idealized models of the flow over an airfoil pitching continuously (Flow D) or pitching up to some positive angle of incidence and then being held at rest (Flow E).

In both Flows C and D, the initial conditions at $t = 0$ correspond to steady flow past a flat plate. Then, as t increases the retardation of the external flow becomes progressively stronger, and the wall shear stress, τ_w, at the trailing edge decreases. At some instant of time, τ_w reaches zero at $x = 1$, and from that instant onward, a region of reversed flow, of increasing extent, would develop on the plate. The value of ωt ($= -\partial U_e/\partial x$), at the instant when $\tau_w = 0$ at $x = 1$ is a measure of the relative ability of that particular boundary layer to be retarded without suffering flow reversal.

There is some *steady*, linearly retarded flow that will just provoke separation at $x = 1$, and the (constant) value of $(-\partial U_e/\partial x)$ corresponding to it can be regarded as an equivalent quasi-steady value of ωt, i.e., for $\omega \to 0$. There will be one such value for the steady flow corresponding to Flow C and a nearly identical one for the flow corresponding to Flow D (the only difference being due to Reynolds number).

Figure 4 shows some results for Flows C and D, in which the value of ωt for $\tau_w = 0$ at $x = 1$, normalized on the appropriate quasi-steady value just described, is plotted as a function of ω. For both flows, the effect of time dependence is to increase the critical value of ωt above the value for $\omega \to 0$, indicating that the unsteady boundary layers are more resistant to flow reversal than the steady ones. In Flow C, $(\omega t)_{\tau_w=0}$ increases to a value some 50% greater than that for quasi-steady separation, and then remains approximately constant for $\omega > 0.6$. In Flow D, the value of $(\omega t)_{\tau_w=0}$ increases continuously with increasing ω, and there is a substantial delay in the onset of flow reversal for large values of ω. For example, with $\omega = 10$, $(\omega t)_{\tau_w=0}$ is some five times greater than it is when $\omega \to 0$ (quasi-steady). At these high values of ω, the streamwise gradients are so large that the validity of the boundary-layer approximations becomes questionable. For this reason, the results for Flow D, with $\omega > 8$, should be treated with caution (shown by dashed curves in Fig. 4). The trend suggests that, for high enough values of ω, vanishing wall shear stress might never occur.

One of the effects of time dependence is to modify the streamwise pressure gradient, $\partial p/\partial x$. For two-dimensional flow, Euler's equation for flow in the external stream takes the form:

$$\partial U_e/\partial t + U_e(\partial U_e/\partial x) + (1/\rho)(\partial p/\partial x) = 0 \qquad (10)$$

The equation shows that $\partial p/\partial x$ can be either increased or decreased, depending on the sign of $\partial U/\partial t$. The quantity R, where

$$R = -(\partial U_e/\partial t)/[(1/\rho)(\partial p/\partial x)] \qquad (11)$$

is a measure of the contribution of $\partial U_e/\partial t$ to the total pressure gradient. Positive values of R correspond to cases where $\partial U_e/\partial t$ increases the adverse pressure gradient; negative values to cases where the adverse pressure gradient is alleviated.

Figure 5 shows the results for Flows C and D plotted vs R. Actually, R is a function of x, and the values plotted correspond to $x = 0.5$. Flow D generates negative values of R, and the delay in the onset of reversed flow takes place in an environment where the adverse pressure gradients are *alleviated* by the effects of time dependence. On the other hand, Flow C generates positive values of R and while the effects are less marked than in Flow D, there is again a delay in the onset of reversal, and it occurs in the face of an *increasingly adverse* pressure gradient. Indeed, at the highest value of ω considered, $\partial p/\partial x$ is some 300 times greater than was necessary to cause separation at $x = 1$ in steady flow.

The inference from Figs. 4 and 5 is that the augmentation or alleviation of $\partial p/\partial x$ does play a part in the effect of time dependence on the onset of flow reversal, but it is clearly not

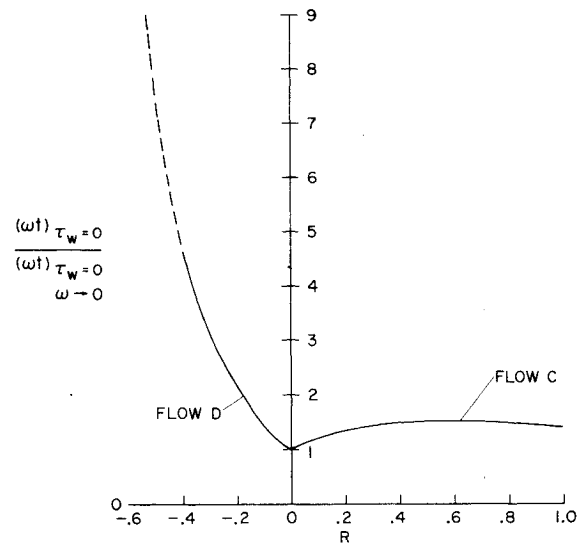

Fig. 5 Variation of velocity gradient magnitude for incipient reversal at $x = 1$ vs pressure-gradient ratio R.

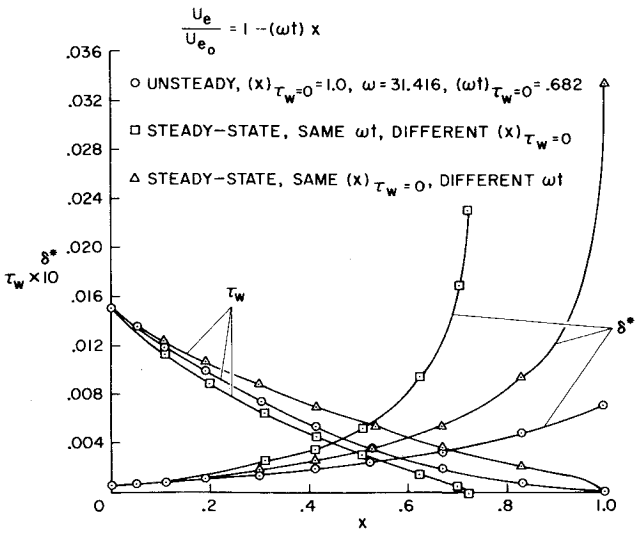

Fig. 6 Wall shear stress and displacement thickness distribution for Flow C.

the only mechanism to be considered and, at least for the flows discussed here, it is not even the dominant one.

Another mechanism by which time dependence makes itself felt is a kind of inertia effect. For flow reversal to occur, the velocity profiles must be distorted from their initial flat-plate form to a form not unlike the steady separation profile. This distortion, which involves disproportionate retardation of the fluid particles near the surface compared with those toward the outer edge of the boundary layer, cannot take place instantaneously but requires a finite time. Thus the distortion lags behind the retardation of the external flow and, by the time the distortion has reached the stage permitting reversed flow at the wall, the retardation of the external stream has progressed further than would have occurred in a steady flow.

The inertia effect just described operates in the direction of delaying the upstream movement of flow reversal regardless of the effect of the unsteadiness on $\partial p/\partial x$. It should be noted further that, regardless of the sign of $\partial U_e/\partial t$ and its effect on $\partial p/\partial x$, the point of vanishing τ_w can move upstream only if $\partial U/\partial t$ is locally negative in the vicinity of the wall.

So far we have examined the delay in flow-reversal onset due to time dependence; it is also of interest to look at the behavior of τ_w and δ^* in the neighborhood of the point where $\tau_w = 0$. Figure 6 shows the variation of τ_w and δ^* with x, for Flow C, at the instant when $\tau_w = 0$ at $x = 1$. Figure 7 shows the corresponding data for Flow D. In both figures, the results of two quasi-steady calculations are also plotted for comparison. In one, the value of ωt (i.e., the value of $-\partial U_e/\partial x$) is the same, and this boundary layer separates ahead of $x = 1$. In the other, the value of ωt is reduced so that separation occurs at $x = 1$. (The reduced value of ωt is the one used to normalize the ordinates in Figs. 4 and 5.)

The levels of τ_w are widely different for the two quasi-steady cases (Fig. 7) as a result of the difference in ωt and its effect on U_e in Flow D. Otherwise, Figs. 6 and 7 illustrate substantially the same features.

The steady-flow separation is associated with steepening of the curve of τ_w vs x, i.e., with negative values of $\partial^2\tau_w/\partial x^2$, the slope, $\partial\tau_w/\partial x$, of course, being negative, too. This steepening of the curve is reminiscent of the square-root singularity observed in the laminar case and is accompanied by a rapid increase in δ^*, again suggesting the existence of a singularity. In contrast, in the time-dependent cases, the approach to zero wall shear stress is more gradual. The first derivative, $\partial\tau_w/\partial x$, naturally remains negative, but the second derivative appears to be positive, i.e., the curve of τ_w vs x becomes less steep as the point of $\tau_w = 0$ is approached. Moreover, the displacement thickness increases less rapidly and remains smaller than it does in the steady case. In short, there is no indication of singular behavior in the approach of the unsteady boundary layer to the point of flow reversal, and there is no indication that the boundary-layer equations would break down at that point. The results thus support the views of Sears and Telionis[10] that flow reversal and the appearance of a singularity in the mathematics are distinct events in an unsteady boundary layer. The work of Sears and Telionis would indicate that for flows similar to C and D, in which the point of flow reversal is moving upstream, the singularity should lie farther downstream than the point where $\tau_w = 0$. The singularity is the mathematical expression of separation, or flow detachment from the body and, accordingly, the separation point would also be expected to lie downstream of the point of flow reversal. It was not possible to continue the calculations beyond the point of instantaneously zero wall shear stress, and so the existence of a singularity downstream of this point could not be verified directly. Calculations could not be done easily for the situation where the point of zero τ_w is moving *downstream*. For this case, the Sears-Telionis model would predict that the singularity lies upstream of the point of flow reversal.

Flow E, it will be recalled, is initially identical to Flow D, but subsequently relaxes to steady-state equilibrium after the external flow is frozen at a particular value of ωt. Since the effect of time dependence is to delay the onset of flow reversal, the relaxation process is usually accompanied by an upstream movement of the

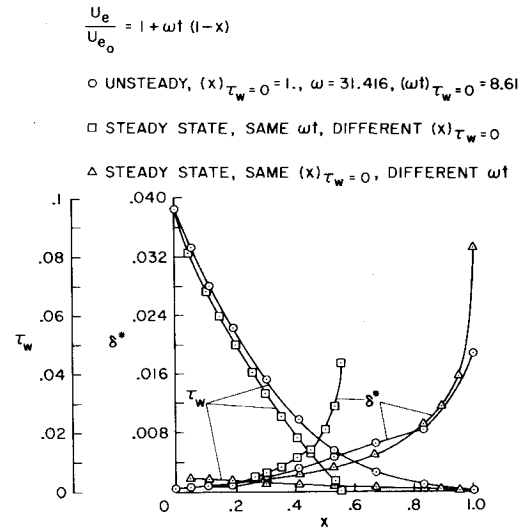

Fig. 7 Wall shear stress and displacement thickness distribution for Flow D.

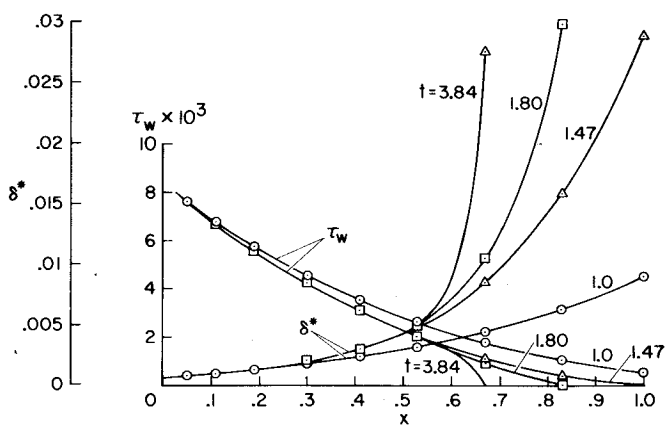

Fig. 8 Development of displacement thickness and wall-shear stress for Flow E ($\omega = 1.57$, frozen when $t = 1.0$).

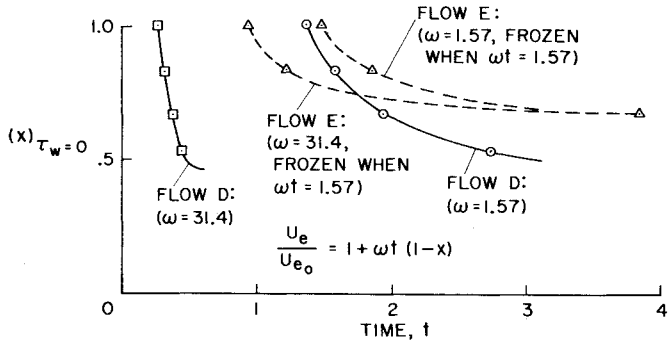

Fig. 9 Upstream movement of the point of flow reversal, Flows D and E.

point of zero wall shear stress. Also, the characteristics of the flow have to change from those appropriate to time-varying conditions to those appropriate to steady-state conditions. This process is illustrated in Fig. 8, which shows the variation of τ_w and δ^* with x and t for Flow E with $\omega = 1.57$. The shapes of the $\tau_w(x)$ curves reflect a change from positive to negative values of $\partial^2\tau_w/\partial x^2$ in the neighborhood of $\tau_w = 0$. At the same time, the curves of δ^* vs x become steeper as the point of zero τ_w is approached. Thus there is clear evidence of the re-establishment of the singular, or near-singular, behavior associated with the steady-flow separation phenomenon.

In flows such as Flow D, the rate at which the point of zero wall shear stress moves upstream is strongly dependent on (although less than proportional to) the rate of distortion of the external flow. Figure 9 shows the effect of increasing ω by a factor of 20. During the relaxation phase of Flow E, however, the point of flow reversal moves forward toward the steady-state separation point in the absence of further distortion of the external flow. It appears, in fact, that the rate of forward movement is substantially independent of the value of ω corresponding to the initial distortion of the flow (Fig. 9). Note the comparatively long time necessary for the flow to settle down to the new steady-state situation, nearly 4 time units, which (at this value of ωt) is roughly five times the time taken for a fluid particle in the external flow to be convected from $x = 0$ to $x = 1$. Thus, it would seem that the steady-state equilibrium is not reached until virtually all the fluid in the boundary layer has been convected off the plate and replaced by new fluid that has crossed the leading edge after freezing of the external flow.

Discussion and Conclusions

In the boundary layer on a flat plate, in an oscillating stream, flow reversal at the wall can occur during part of the cycle if the amplitude or frequency is high enough. Reversal, in this case, can be explained in terms of strong, instantaneous positive pressure gradients associated with the time dependence. Since the wall shear stress can never fall to zero in steady flow over a flat plate, this result illustrates the *promotion* of flow reversal by the effects of time dependence.

In contrast, in the other types of unsteady turbulent flow examined, including oscillatory *retarded* flow and two monotonically varying retarded flows, time dependence always had the effect of *delaying* the onset of flow reversal. When the time dependence was associated with an *alleviation* of the adverse pressure gradients, the delay was large. However, and this is highly significant, a small delay occurred even when the pressure gradients were augmented, indicating that pressure gradient is not the only causal link between time dependence and the effect on flow-reversal onset that it produces.

In addition, the flow possesses a kind of inertia that limits the rate of distortion of the velocity profiles which is a necessary part of the approach to flow reversal. This distortion lags behind the retardation of the external flow that causes it, and the retardation is correspondingly greater, by the time reversal occurs, than it would be under steady-state conditions. When the pressure-gradient effect and the inertia effect reinforce one another, as in the present Flow D, then the delay in reversal onset is substantial. When the effects oppose one another, as in Flows B and C, the delay is smaller but the inertia effect is evidently dominant. The exception is the oscillatory flat-plate flow (Flow A) where the pressure-gradient effect appears to dominate. However, the absence of separation in the steady analog of this flow makes it difficult to assess the significance of the inertia effect.

The inertia effect also arises in the relaxation of an initially unsteady flow toward steady-state equilibrium following freezing of the external velocity distribution. This relaxation is a relatively slow process and is not complete until virtually all the fluid in the original time-dependent flow has been convected away and replaced by new fluid that has entered the boundary layer after freezing of the external flow.

The approach to zero wall shear stress is characteristically different, in a time-dependent flow, from the familiar pattern in steady flow. In unsteady flow in a prescribed external velocity distribution, there is no evidence of singular behavior in either the wall shear stress or the displacement thickness. The curve of τ_w vs x does not steepen as the point of zero τ_w is approached as it would in a steady flow due to the square-root singularity, but appears to become less steep in the time-dependent flow: $\partial\tau_w/\partial x$ is negative, while $\partial^2\tau_w/\partial x^2$ is positive. According to the model of Sears and Telionis, a singularity would be expected to occur downstream of the point of flow reversal in the types of flow considered here. It is this singularity that is associated with separation, in the sense of detachment of the external stream from the body surface. Flow reversal and separation are distinct events in an unsteady flow, and their points of onset do not coincide as they would in steady two-dimensional flow. If separation does indeed occur downstream of the point of flow reversal, in the flows discussed here, then the delay in boundary-layer *separation* due to time dependence is even greater than the delay in reversal indicated by the present results.

Quasi-steady methods have limited usefulness in the calculation of time-dependent, turbulent boundary layers. Quasi-steady predictions of displacement thickness are not even tolerably adequate over the range of frequencies, or rates of change, considered here. The corresponding predictions of wall shear stress are close to the time-dependent values so long as the wall shear stress does not become too small. When the condition of incipient flow reversal is approached, quasi-steady calculations fail to predict either the correct point of reversal or the correct behavior of the flow in the neighborhood of this point. It has sometimes been suggested that quasi-steady methods can be improved by artificially increasing or decreasing the pressure gradient by the amount of the term $\partial U_e/\partial t$ in the momentum equation. This procedure is misleading because, as we have noted, the pressure gradient is not the only mechanism, or necessarily the dominant one, by which the effects of time dependence make themselves felt. Indeed, in flows such as Flows B and C, manipulating the pressure gradient in the manner described would lead to prediction of the effects of unsteadiness which are *opposite* to those obtained using the full unsteady boundary-layer equations.

References

[1] Hicks, J. G. and Nash, J. F., "The Calculation of Three-Dimensional Turbulent Boundary Layers on Helicopter Rotors," CR-1845, May 1971, NASA.

[2] Patel, V. C. and Nash, J. F., "Some Solutions of the Unsteady Turbulent Boundary Layer Equations," *Recent Research on Unsteady Boundary Layers* (*Proceedings of the IUTAM Symposium*, Quebec 1971), edited by E. A. Eichelbrenner, Presses de l'Université Laval, Quebec, 1972.

[3] McDonald, H. and Shamroth, S. J., "An Analysis and Application of the Time-Dependent Turbulent Boundary-Layer Equations," *AIAA Journal*, Vol. 9, No. 8, Aug. 1971, pp. 1553–1560.

[4] Singleton, R. E., Nash, J. F., Carr, L. W., and Patel, V. C., "Unsteady Turbulent Boundary-Layer Analysis," TM X-62, 242, Feb. 1973, NASA.

[5] Singleton, R. E. and Nash, J. F., "A Method for Calculating Unsteady Turbulent Boundary Layers in Two- and Three-Dimensional Flows," *Proceedings of the AIAA Computational Fluid Dynamics Conference*, July 1973, AIAA, Palm Springs, Calif.

[6] Nash, J. F. and Patel, V. C., "A Generalized Method for the Calculation of Three-Dimensional Turbulent Boundary Layers," *Fluid Dynamics of Unsteady, Three-Dimensional and Separated Flows*, Proceedings of Project SQUID Workshop, Georgia Institute of Technology, Atlanta, Ga., June 1971.

[7] Nash, J. F. and Patel, V. C., *Three-Dimensional Turbulent Boundary Layers, SBC Technical Books*, Sybucon, Inc., Atlanta, Ga., 1972.

[8] Bradshaw, P., Ferriss, D. H., and Atwell, N. P., "Calculations of Boundary-Layer Development Using the Turbulent Energy Equation," *Journal of Fluid Mechanics*, Vol. 28, 1967, p. 593.

[9] Bradshaw, P., "Calculation of Boundary Layer Development Using the Turbulent Energy Equation, VI, Unsteady Flow," NPL Aerospace Rept. 1288, Feb. 1969, National Physical Laboratory, England.

[10] Sears, W. R. and Telionis, D. P., "Unsteady Boundary-Layer Separation," *Recent Research on Unsteady Boundary Layers (Proceedings of the IUTAM Symposium*, Quebec 1971), edited by E. A. Eichelbrenner, Presses de l'Université Laval, Quebec 1972.

FEBRUARY 1975 AIAA JOURNAL VOL. 13, NO. 2

Penetration of a Lateral Sonic Gas Jet into a Hypersonic Stream

WILLIAM G. REINECKE*
Avco Systems Division, Wilmington, Mass.

Experiments were conducted to measure the extent of the disturbance caused by large lateral sonic gas injection from a slender cone into a Mach 13 airstream. The variables in the tests were injectant gas, injectant mass flow, nozzle geometry, and freestream pressure altitude (or jet pressure ratio). The measured dependent variables were the jet penetration height and the height of the resultant shock wave in the freestream. Within the variable ranges tested the data showed that the jet behaved as a point source and that the nozzle cross-section shape was unimportant. The measured jet penetration heights were compared with the predictions from four formulae available in the literature. The formula of Zukoski and Spaid predicted the jet penetration height very well. In addition, it was shown that the local height of the shock in the freestream resulting from the injection could be predicted reasonably well, and in a manner consistent with the Zukoski and Spaid model, by considering the shock to be the result of a sphere placed in the freestream at the jet location having a radius equal to the jet penetration height.

Nomenclature

D_j = jet throat diameter
h = penetration height, jet shock height
k = the coefficient $h/r(\bar{m})^{1/2}$
m = injectant mass flow rate
$\bar{m}$ = $m/\rho_\infty u_\infty \pi r^2$
p_j^o = injectant gas total pressure
R = universal gas constant
r = cone base radius
s = interaction shock height
T_j^o = injectant gas total temperature
T_∞^o = freestream total temperature
u_∞ = freestream speed
$\mathcal{M}_j$ = injectant gas molecular weight
$\mathcal{M}_\infty$ = freestream molecular weight
γ_j = injectant gas specific heat ratio
ρ_∞ = freestream density

THE purpose of the tests and correlation described herein was to determine the size disturbance that can be produced by the discrete injection of a gas laterally into a hypersonic stream. Specifically, we wished to measure the height above the cone surface of the shock wave caused by large lateral gaseous injection and the variation of this height with jet characteristics and to assess the accuracy of various analytical models in predicting the shock height. The independent variables in the tests were the mass flow, injectant gas, injector nozzle geometry, and pressure altitude. The test geometry, Mach number, and injectant stagnation temperature (about 70°F) and pressure (about 50 psia) were fixed. The model was a 6° half angle cone, 0.5 in. in base radius with variable geometry sonic injection nozzles located 180° apart and 0.20 in. forward of the cone base plane. The axes of the jets were normal to the cone centerline. The sizes of the interactions on the opposite sides of the cone were independent at even the highest injection rates. This was observed in preliminary tests in which gas was injected at a constant rate on one side of the cone while the injection rate on the other side was varied from zero to maximum.

The test conditions are given in Table 1. The tests were conducted in Avco's 20 in. diam shock tunnel and most of the data were obtained at Mach 13.2 and at 151,000 ft pressure altitude. The corresponding freestream Reynolds number based on cone base radius was 52,700. At this condition three injector nozzle cross-sectional geometries were used (circles, and 5 and 10 to 1 rectangles with their longer sides normal to the exterior flow direction), and four different gases were injected (N_2, Xe, He, and Freon 116) at various mass flow rates. The injectant mass flow rate was controlled by the jet throat area. The tests at 168,000 and 195,000 ft pressure altitude were conducted with nitrogen flowing from slot nozzles only and were directed at determining the effect, if any, of injectant stagnation to freestream pressure ratio (or altitude) independent of the other test variables.

Received February 13, 1974; revision received August 23, 1974. This work was supported by the U.S. Air Force Systems Command, Space and Missile Systems Organization under Contract F04-701-71-C-0002.

Index categories: Jets, Wakes, and Viscid-Inviscid Flow Interactions; Supersonic and Hypersonic Flow.

* Senior Consulting Scientist. Associate Fellow AIAA.